Detection of Linear Hyperintensity Objects on High Resolution T2 Enhanced Images

S-I. Urayama[1], M. Hiroki[1], N. Sugimoto[2], T. Hanakawa[1], H. Fukuyama[1], M. Abe[3]

[1]Human Brain Research Center, Kyoto University, Kyoto, Japan, [2]Dept. Systems Science, Kyoto University, Uji, Japan, [3]Dept. Zoology, Kyoto University, Kyoto, Japan

Introduction

Linear Hyperintensity Objects (LHOs), which are sometimes recognized in the cerebral white matter on T2-weighted MR images (Fig.1), had never been studied from the clinical viewpoint. Recently, strong relation between LHOs and hypertension was reported [1,2] and it was suggested that LHOs have a potential as an indicator for hypertensive small vessel disease. However, the width of LHOs is too small (generally 1 or 2 pixels) to adapt conventional linear object detection algorithms because of severe partial volume effect even on a high resolution image and limitation of smoothing. On the other hand, LHOs has several characteristics, i.e., its width of at most 1.2 mm, almost straight shape, no branch structure, and radial divergence on a transverse image. In this study, LHOs detection was carried out based on shape analysis with subpixel resolution and characteristic matching.

Materials and Methods

T2-weighted images were taken with a 3T whole body scanner Trio (Siemens, Germany). The imaging parameters were; sequence : TurboSpinEcho, TR : 7000 msec, TE : 102 msec, FOV : 182x220 mm, image matrix : 426x512 pixel, pixel size : 0.429x0.429 mm, slice thickness : 3 mm.

The LHOs detection algorithm is consisted of three steps; 1. ridge line detection with pixel resolution, 2. ridge shape analysis with subpixel resolution, and 3. LHOs selection using the results of the step 2. Before describing the detail of each step, continuous image derived from the original discrete one is defined because the continuous one is used not only subpixel analysis but also definition of the first and second derivative images used in the step 1. For the definition, four conditions are considered; 1. the first and second derivative image must be continuous, 2. no oscillation in the interpolation is guaranteed because it can be a pseudo ridge line, 3. minimum smoothing is allowed because of denoise, 4. discrepancy of the intensities at a pixel center on both continuous and discrete images is allowed. In this study, we define the continuous image $f_c(x,y)$ by applying gaussian smoothing to the zero-order-hold image of a discrete one $f(x_i,y_i)$ (Eq.1, Fig.2).

$$f_c(x,y)\equiv\sum_{x_i y_i} f(x_i,y_i)\cdot\int_{y_i-y-0.5}^{y_i-y+0.5}\int_{x_i-x-0.5}^{x_i-x+0.5}\exp\left(-\frac{x'^2+y'^2}{2\sigma^2}\right)dx'dy'=\sum_{x_i y_i} f(x_i,y_i)\cdot G(x_i-x)\cdot G(y_i-y) \qquad \left(G(s)\equiv\int_{s-0.5}^{s+0.5}\exp\left(-\frac{s'^2}{2\sigma^2}\right)ds' : \text{numerically calculated}\right) \quad (1)$$

The ridge line detection algorithm in the step 1 is based on quadratic approximation using Taylor expansion (Eq.2). Using the eigenvalues $\lambda_i\ (|\lambda_1|\ge|\lambda_2|)$ and eigenvectors $\mathbf{v}_i\ (|\mathbf{v}_i|=1)$ of the Hessian **H**, the quadratic equation can be expressed with sum of two parabola functions, denoted with an underline in Eq.2, in a coordinate system **dx**' defined by $\mathbf{v}_i$. If a ridge line runs in a pixel, $\lambda_1<0$ and the vertex of the first parabola is inside of the pixel, i.e., the position apart from the pixel center by $|(\nabla f_c\cdot\mathbf{v}_1)/\lambda_1|\mathbf{v}_1$ must be inside. Hence, pixels which satisfy these two conditions are detected as ridge line pixels (RLPs).

$$f_c(\mathbf{x}+\mathbf{dx})\cong f_c(\mathbf{x})+\nabla f_c\cdot\mathbf{dx}+0.5\cdot{}^T\mathbf{dx}\cdot\mathbf{H}\cdot\mathbf{dx} \;\Rightarrow\; 0.5\cdot\left\{\underline{\lambda_1\left(dx'_1+(\nabla f_c\cdot\mathbf{v}_1)/\lambda_1\right)^2}+\underline{\lambda_2\left(dx'_2+(\nabla f_c\cdot\mathbf{v}_2)/\lambda_2\right)^2}\right\}+f_c(\mathbf{x})-0.5\cdot\sum_{i=1}^{2}(\nabla f_c\cdot\mathbf{v}_i)^2/\lambda_i \quad (2)$$

In the ridge shape analysis in the step 2, the intensity, curvature and line direction at the nearest ridge line point from the center of RLPs and the width of ridge line, are estimated. At first, the profile and its first and second derivative values along the $\mathbf{v}_1$ direction from the pixel center are calculated with 0.1 pixel interval. The nearest ridge point, at which the first derivative becomes 0, is estimated with the linear interpolation and then the intensity, curvature (given by λ_1) and line direction (given by $\mathbf{v}_2$) are calculated. The width of ridge line is defined by the distance of two points at which the second derivatives become 0.

In the step 3, LHOs are selected from all RLPs using the information gotten in the step 2. Since partial volume effect has been eliminated in the intensity image, simple thresholding can be removed RLPs in the celebro-spinal fluid (CSF) region. On the width image, RLPs whose value is larger than 1.5 mm are also removed. On the direction image, remaining RLPs are segmented to separate linear shape objects by region growing technique with threshold of ±30 deg, and then segmented object, which satisfies that the number of pixels is less than 10 or that the difference between its average direction and the radial direction diverging from the image center is more than 45 deg, is also removed. The average curvatures of the remaining objects are calculated and superimposed on the original image.

Results and Discussion

Figure 3 shows the resultant images of the step 2 and 3. Although all ridge like structure are detected only by the step 1 process, almost LHOs can be selected well by combining with subpixel shape analysis. However, LHOs which run in parallel with very small intervals are difficult to detect because the gaussian smoothing in Eq.2 fills up the intervals. In addition, ridge line width is tend to overestimate because of the smoothing. Therefore, another sophisticated smoothing like object direction sensitive filter is necessary. In future work, we will try to extend this method to 3-dimensional images.

References [1] M.Hiroki, et al., Cerebrovasc Dis., 13, pp.242-250, 2002; [2] M.Hiroki, et al. Proc. Cerebrovasc Di s., 2003, 16 (suppl. 4):S117, 2003

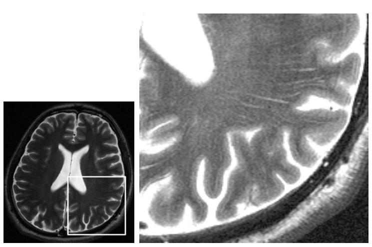

Fig.1

T2 enhanced image used for the LHOs detection. LHOs are clearly observed in the rectangular areas.

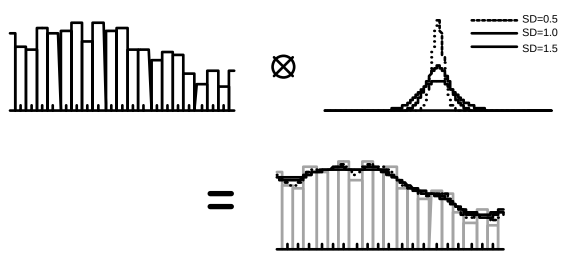

Fig.2

Schema describing the definition of continuous image. The original discrete image is considered 0-order-hold one and gaussian smoothing is applied to it.

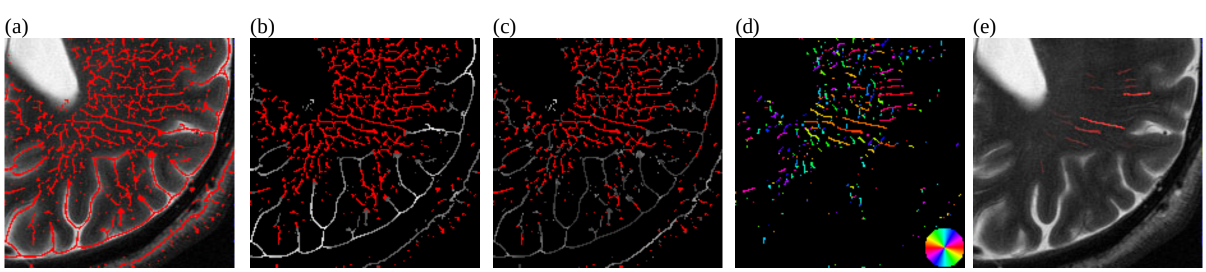

Fig.3 The resultant images of (a) RLPs detection, (b) intensity estimation, (c) width estimation, (d) direction estimation and (e) average curvature on the original image, respectively. Red pixels in (b) and (c) are remained after the thresholds. Colored circle in (d) shows the direction look-up-table. The parameter σ in Eq.2 was set to 1.5 pixel.